Polymer 51 (2010) 5432–5439

Contents lists available at ScienceDirect

Polymer

journal homepage: www.elsevier.com/locate/polymer

Synthesis, characterization and fine-tuning of bimodal poly(organosiloxane) nanoparticles

C. Scherer [a,b], S. Utech [a,c], S. Scholz [a], S. Noskov [a], P. Kindervater [d], R. Graf [d], A.F. Thünemann [b], M. Maskos [a,b,*]

[a] Institut für Physikalische Chemie, Universität Mainz, Jakob-Welder-Weg 11, 55128 Mainz, Germany
[b] BAM Federal Institute for Materials Research and Testing, Unter den Eichen 87, 12205 Berlin, Germany
[c] Institut für Mikrotechnik Mainz GmbH (IMM), Carl-Zeiss-Straße 18-20, 55129 Mainz, Germany
[d] Max-Planck-Institute for Polymer Research, Ackermannweg 10, 55128 Mainz, Germany

ARTICLE INFO

Article history:
Received 28 June 2010
Received in revised form
20 August 2010
Accepted 25 September 2010
Available online 12 October 2010

Keywords:
Nanoparticles
Polyorganosiloxane
Field-flow fractionation (FFF)

ABSTRACT

The acid catalyzed sol–gel type synthesis of polyorganosiloxane core-shell nanoparticles with removable PDMS core in aqueous dispersion leads to the inherent formation of a bimodal size distribution with smaller spheres having approximately 26 nm radii and larger nanoparticles with 60 nm in radius. The origin of the self-organized bimodality is investigated and finally attributed to a combination of stabilization of the growing particles due to i) a miniemulsion-type stabilization by the ultrahydrophobe PDMS and ii) by surface co-stabilization by the employed surfactant. The significant influence of temperature, pH, stirrer speed and amount of the surfactant on the particle sizes allows for the design and fine-tuning of different nanoparticles sizes and distributions.

1. Introduction

Increasing research activities have taken advantage of nano- and microparticle technology in such fields as drug and gene delivery, [1–6] optical, [7,8] catalysis, [9] electronic, [10,11] chromatography [12] and magnetic [13,14] applications. Among the different materials employed, silica-based polymeric materials are of major importance. Methods, such as the Stöber process [15,16] have been developed to produce monodisperse spherical silica particles that range in size from nano- to millimeters. These broad addressable size range, coupled with the ability to modify the surface with organics, are key factors that contribute to their utility and importance.

In this paper, we present a chemical system based on poly (organosiloxane)s. First, the organosilane monomers are hydrolyzed and condensed via the sol–gel process in aqueous dispersion in the presence of a surfactant. Sequential addition of the monomers leads to the formation of spherical core-shell colloids with diameters of 5 nm up to about 100 nm, depending on the experimental conditions. The particles are then transferred into an organic solvent and, after saturation of the reactive surface groups, can be isolated and are redispersable in organic solvents. This approach has the advantage that one can control (i) the size of the particles, (ii) the thickness and number of shells, (iii) the network density, as well as (iv) the internal architecture, which can finally be used to generate hollow nanoparticles [17–21]. The incorporation of additional functional groups on the surface of the particles opens the possibility to further modify the surface properties of the nanospheres, e.g. hydrido-silane functionalities ($R_3Si–H$) can be used for subsequent coupling of heterotelechelical end-functionalized poly(ethylene oxide) PEO via a hydrosilation reaction to form water soluble nanoparticles [22]. The introduction of hydridosilane functionalities requires an acid catalyzed synthesis route.

For potential biological applications such as drug delivery or drug release systems, the control and fine-tuning of the size and polydispersity of the nanoparticles are of particular interest. In addition, hollow nanoparticles allow for the potential capability of increased encapsulation. Finally, the possibility to introduce and modify functional groups on the nanoparticle surface is of additional importance.

2. Materials and methods

2.1. Materials

Water was purified with a milli-q deionizing system (Waters, Germany). Trimethoxymethylsilane (T), diethoxydimethylsilane (D),

* Corresponding author. BAM Bundesanstalt für Materialforschung und -prüfung, Unter den Eichen 87, 12205 Berlin, Germany. Tel.: +49 30 81041619.
E-mail address: Michael.Maskos@bam.de (M. Maskos).

0032-3861/$ – see front matter © 2010 Elsevier Ltd. All rights reserved.
doi:10.1016/j.polymer.2010.09.065

ethoxytrimethylsilane (M), hexadimethylsilazane (HMN) (Wacker Chemie, Germany), tetrahydrofurane, toluene, methanol (Merck, Germany), sodium hydroxide, TWEEN 20 (Fluka, Germany), benzethonium chloride ([2[2(p-1,1-3,3-tetramethylbutylphenoxy)ethoxy] ethyl]ammonium chloride, Aldrich, Germany) and (p-chloro-methylphenyl)trimethoxysilane (ClBz-T), Polydimethylsiloxane (PDMS, $M = 1250$ g/mol), Octamethylcyclotetrasiloxane (D4), and Decamethylcyclopentasiloxane (D5, all ABCR, Germany) were used as received.

2.2. Synthesis

The synthesis and characterization of poly(organosiloxane) nanospheres with different particle topologies are described in detail in ref. [17]. The synthesis is based on the hydrolysis and co-condensation of dialkyldialkoxysilanes (D) and alkyltrialkoxysilanes (T) in aqueous dispersion at room temperature, if not stated otherwise, by sequential addition of monomer mixtures in the presence of a surfactant. Saturation of reactive silanol or silanolate groups by reaction with monoalkoxysilanes prevents the irreversible aggregation of the particles and allows the transfer into toluene as redispersable nanoparticles. For the synthesis of hollow particles, D units are first condensed to chains and prevented from reacting with subsequently added monomer by the addition of monoalkoxysilanes. By the use of mixtures of D and T in the formation of the shells, these chains can later on diffuse out of the interior after transfer into toluene and can be removed by ultrafiltration. Fig. 1 shows the reaction scheme to obtain hollow poly (organosiloxane) nanospheres.

2.3. Core-shell-shell spheres with PDMS core not attached to the surrounding shell (hollow spheres). aqueous dispersion, base catalyzed route

8 g (54 mmol) of diethoxydimethylsilane (D) for the core was added dropwise to a solution of 125 g of water, 600 mg of 10% (w/w) sodium hydroxide (1.5 mmol), and 2.0 g benzethonium chloride (4.46 mmol) through a syringe pump over 1 h under continuous mechanical stirring ($U = 300$ rpm) at room temperature (293 K). The dispersion was stirred overnight, and subsequently, 100 mg (0.96 mmol) of ethoxytrimethylsilane (M) was added to saturate the reactive chains. After 8 h, another 100 mg (0.96 mmol) of M was added, and the dispersion was stirred overnight to complete the reaction. The monomer mixture for the first shell was added according to Table 1 at 7 mL/h. After 1 week of stirring, the addition of the monomer mixture for the second shell was performed dropwise (9.9 mL/h), and the dispersion was stirred overnight.

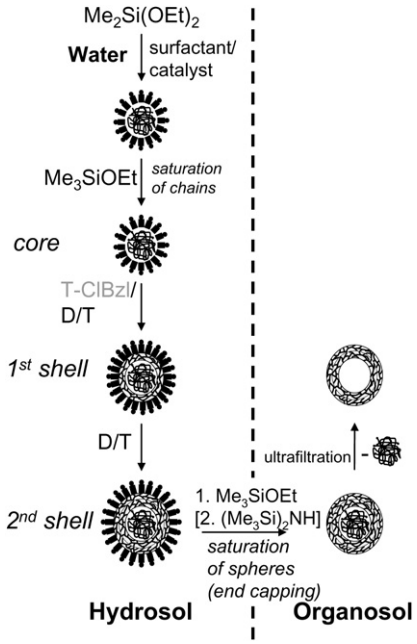

Fig. 1. Schematic representation of the synthesis of hollow spherical polyorganosiloxane nanoparticles; D: chain forming monomer, T: network forming monomers.

2.4. End capping

In order to partially saturate the still reactive surface groups of the nanoparticles, 5 g (42.0 mmol) of M were added to 25 g of the nanoparticles dispersion and stirred overnight. Subsequently, another 2.5 g (21.0 mmol) of M were added and stirred for 5 h. The particles were precipitated by addition of methanol, isolated by filtration (Rotilabo folded cellulose filters type 113P, retention range 5–8 μm) and transferred into 50 mL toluene. After evaporation of residual water and methanol, 1.6 g (9.9 mmol) of hexamethyldisilazan (HMN) were added and stirred for 5 h to complete the end capping. After precipitation in methanol and subsequent drying, the material was redispersed in THF, and the PDMS chains were removed by ultrafiltration (regenerated cellulose membrane, MWCO = 30 kDa). The complete removal was checked by GPC.

2.5. Aqueous dispersion, acid catalyzed route

5 g (34 mmol) of diethoxydimethylsilane (D) for the core was added dropwise to a solution of 125 g of water and 5 g of 10% (w/w) dodecylbenzenesulfonic acid (DBS) (1.5 mmol) through a syringe pump over 1 h under continuous mechanical stirring ($U = 300$ rpm) at room temperature (293 K). The dispersion was stirred overnight, and subsequently, 100 mg (0.96 mmol) of ethoxytrimethylsilane (M) was added to saturate the reactive chain ends. After 8 h, another 100 mg (0.96 mmol) of M was added to complete the reaction, and the dispersion was stirred overnight. The monomer mixture for the first shell was added according to Table 1 at 8 mL/h. After 4 h of stirring, the addition of the monomer mixture for the second shell was performed dropwise (8 mL/h), and the dispersion was stirred overnight. The end capping was performed as described above using M.

3. Methods

3.1. Circular asymmetrical flow field-flow fractionation (CAFFFE) system

CAFFFE measurements were performed using a CAFFFE channel with Flowbox P2.1 (ConSenxus), a 0.5 mL sample loop, a Bronckhorst Hi-Tec Liqui-Flow delivering the cross-flow, a SFD degasser GT-152, a valve box, and a controller [23]. An analytical UV detector UV/VIS 150 (ThermoFinnigan) operating at 254 nm monitored the

Table 1
Amount of monomers (Chloromethylphenyltrimethoxysilane ClBz-T, methyltrimethoxysilane T, diethoxydimethylsilane D) employed in the synthesis.

sample	monomer ClBz-T/g	monomer T/g	monomer D/g
basic first shell	3	2	2
basic second shell	–	7	3
acidic first shell	3	2	7
acidic second shell	–	6	2

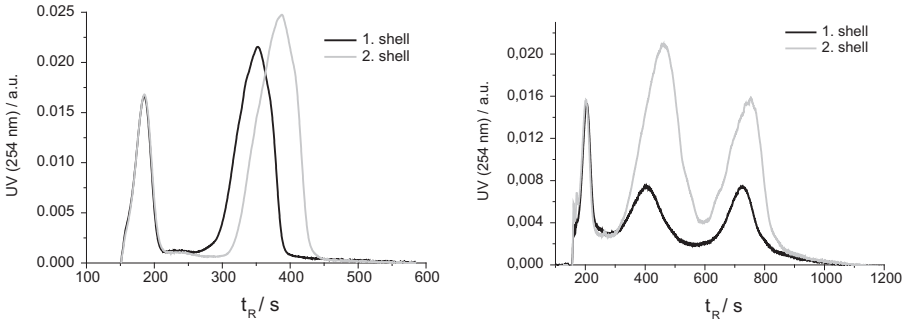

Fig. 2. AF-FFF elution profiles of a) base catalyzed and b) acid catalyzed polyorganosiloxane particles as observed by UV detection ($\lambda = 254$ nm).

eluting particles. Polyethersulfone membranes (MWCO 4 kDa, ConSenxus) were utilized as accumulation walls. Degassed Milli-Q water with NaCl (1 mmol/L) and Tween 20 (100 mg/L) was used as eluent. The flow conditions were 6 mL/min for the channel outlet flow and the cross-flow was decreased from 6 to 0.3 mL/min within 940 s. The samples were diluted with water (1:10, v/v), before injection.

3.2. Asymmetrical flow field-flow fractionation (AF-FFF)

AF-FFF measurements were obtained using an AF-FFF system from Consenxus GmbH equipped with an AF-FFF channel with PMMA cover plate, a 190 μm Mylar spacer, a Thermoseparations constametric 3200 flow pump running at 3 mL/min, a Knauer WellChromMicroStar K-100 injection pump operating at 0.1 mL/min, a 20 μL injection loop, a Bronkhorst HiTec Liqui-Flow, a degasser ERC-3114, valve box, and controller. A Waters 486-UV detector operating at 254 nm and a Dark-II-light scattering detector (110°) from Consenxus monitored the eluting particles. Polyethersulfon membranes were utilized as accumulation walls (MWCO 4 kDa). Degassed Milli-Q water with NaCl (5 mmol/L) and TWEEN 20 (100 mg/L) was used as eluent. The flow conditions were 1 mL/min for the channel outlet flow and the cross-flow was decreased from 2 to 0 mL/min within 1050 s. The samples were diluted with water (1:100, v/v), before injection.

3.3. Gel permeation chromatography (GPC)

GPC was performed in degassed toluene utilizing a Hitachi L-2130 pump operating at 1 mL/min, styrene/divinyl-copolymer columns (MZ Analysentechnik, pore size 10^6, 10^5, 10^4 and 10^3 Å), and a Waters 410 refractive index detector.

3.4. Dynamic light scattering (DLS)

Dynamic light scattering was performed with an argon ion laser (Stabilite 2060-04, $\lambda = 514$ nm, Spectra-Physics), a SP-125 goniometer, and an ALV-5000 multiple-tau digital correlator at angles between 30 and 150° in steps of 30°. The temperature was kept constant at 293 K. The aqueous samples were filtered through Millex-LCR filters (0.45 μm) and the organic solutions through Millex-FG (0.2 μm, Millipore). The DLS data were analyzed by a cumulant fit and by a biexponential fit utilizing the simplex algorithm, respectively, to yield the angular dependent diffusion coefficient D_q. The extrapolation to zero scattering angle gives the apparent diffusion coefficient D which is translated into the appropriate hydrodynamic radius via the Stokes–Einstein relation $R_h = kT/(6\pi\eta D)$, where k is the Boltzmann constant, η the solvent viscosity and T the temperature.

3.5. MALDI-TOF mass spectrometry

The measurements have been performed using a Micromass TOFSpec E mass spectrometer in linear mode. The matrix was nitrophenyloctylether and silver trifluoroacetate has been added to the THF sample solution. After mixing, a droplet was deposited onto the sample holder and the sample was measured after solvent evaporation.

3.6. Gas chromatography

The measurements have been done with a 1 μL sample solution in dichloromethane in a 5080_2 N instrument.

3.7. ^{29}Si-NMR

The measurements of the aqueous dispersions have been performed with a Bruker Advanced 300 MHz spectrometer.

4. Results and discussion

It has been shown before that the synthesis of core-shell-shell nanoparticles with removable polydimethylsiloxane (PDMS) core in order to obtain hollow spheres can be performed by base catalyzed hydrolysis of alkoxysilanes [17]. In order to introduce surface near hydrido functionalities, the reaction conditions have to be changed to acid catalyzed conditions, which is also basically suited to synthesize polyorganosiloxane nanoparticles [22]. The major difference is related to the reaction kinetics of hydrolysis and condensation. E.g., for phenyl-bis(2-methoxyethoxy)silanol, the hydrolysis under acidic conditions (pH 2–3) is reported to be faster compared to the condensation, leading to the formation of small nuclei which aggregate to form the cores of subsequently growing particles [24]. Under basic conditions, the reaction kinetics are inverted leading to small nuclei that steadily grow upon subsequent monomer addition. For the base catalyzed reaction, 10% (w/w) sodium hydroxide is used as catalyst and benzethonium chloride as surfactant while in the acidic route, dodecylbenzenesulfonic acid is

Table 2
Radii of the particles determined by AF-FFF, DLS and TEM after condensation of the first (R_{h1}, R_1) and second shell (R_{h2}, R_2) for base and acid catalyzed polyorganosiloxane particles.

sample		AF-FFF		DLS	TEM	
		R_{h1}/nm	R_{h2}/nm	$R_{h,app}$/nm	R_1/nm	R_2/nm
base catalyzed	1. shell	14.2		14.1		
	2. shell	17.1		17.4	15.0	
acid catalyzed	1. shell	22.5	52.2			
	2. shell	26.6	55.4		23.0	52.0

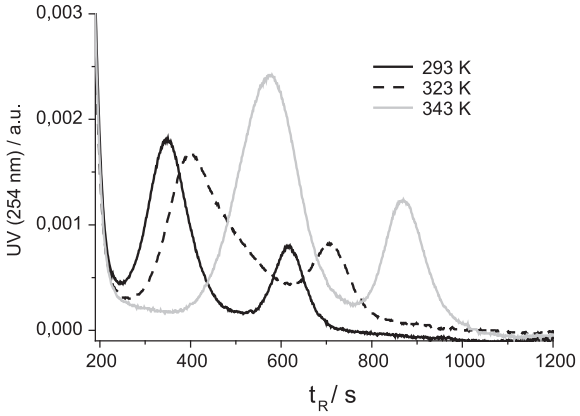

temperature	AF-FFF	
	$R_{h,1}$/nm	$R_{h,2}$/nm
T=20°C	**24.4**	**60.4**
T=50°C	**31.4**	**72.6**
T=70°C	**54.5**	**94.2**

Fig. 3. AF-FFF fractograms after formation of the second shell obtained at different reaction temperatures for acid catalyzed polyorganosiloxane nanoparticles at $U = 300$ rpm, $S = 0.02$ (left) and corresponding radii (right).

used as catalyst and surfactant at the same time. First step in both routes is the condensation of pure diethoxydimethylsilane (D) in aqueous dispersion forming the core. The reactive silanol end groups of the polymer chains are reacted with monofunctional units (ethoxytrimethylsilane, M), followed by the co-condensation of D, methyltrimethoxysilane (T) and p-chloromethylphenyltrimethoxysilane (ClBz-T), forming the first shell. For the second hydrophobic shell, a mixture of D and T is added. After the end capping procedure employing M in order to saturate reactive surface groups, a transfer into organic solvents is possible. At this stage the saturation of reactive surface groups is not quantitative. The residual silanol groups are either reacted with hexamethyldisilazane (HMN) in the base catalyzed way or with M in the acid catalyzed way to ensure the complete saturation which yields in both cases redispersable particles in solvents such as toluene, tetrahydrofurane or chloroform. Depending on the mesh size of the network, the PDMS chains can diffuse out of the nanospheres and are removed by ultrafiltration, leading to the formation of hollow (shell–shell) spheres [25].

4.1. Aqueous dispersion

The characterization of the nanospheres in the aqueous dispersion is particularly difficult due to the presence of free surfactant. In each case, the dispersion is analyzed with asymmetrical flow field-flow fractionation (AF-FFF) and dynamic light scattering (DLS) after formation of the shells. It was not possible to characterize the particle emulsion of the pure PDMS chains (core) with AF-FFF, because the emulsion was not stable even against the relatively low shear forces induced by the flow. In Fig. 2, the fractograms of core-shell-shell spheres obtained with AF-FFF are given. The first peaks in each fractogram are attributed to the void or system peak, which is typically observed in AF-FFF and also present if no sample is injected. The peak maximum determined from AF-FFF normally can be reliably attributed to the average hydrodynamic radius R_h of the particles (typically +/− 5%), whereas unfortunately due to inherent band broadening the size polydispersity can not readily be derived from AF-FFF.

The complete data for the AF-FFF, DLS and TEM analysis are given in Table 2. It should be mentioned that AF-FFF does not yield the mass distribution of the radii, because with applied UV detection only the surfactant covering the surface and the ClBz-T units are detected in combination with the influence of scattering. Nevertheless, the $<1/R_h>^{-1}_z$ average radius obtained by DLS (typically with uncertainties smaller than +/− 5%) is slightly larger as compared to the radius determined by AF-FFF, as expected.

AF-FFF of the basic sample shows a monomodal size distribution, whereas the acid catalyzed sample possesses a bimodal size distribution. Several parameters potentially influencing the appearance of a bimodal distribution are discussed in the following: i) the reaction temperature, ii) the stirrer speed, iii) the fleet ratio S,

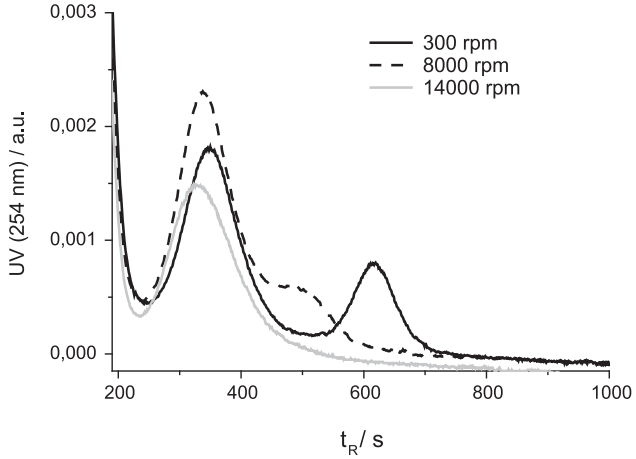

stirrer speed	AF-FFF	
	$R_{h,1}$/nm	$R_{h,2}$/nm
300 rpm	**24.4**	**60.4**
8000 rpm	**23.0**	**41.4**
14000 rpm	**21.8**	-

Fig. 4. Influence of the stirrer speed during the formation of the core of acid catalyzed polyorganosiloxane nanoparticles as analyzed by AF-FFF after formation of the second shell at $T = 293$ K, $S = 0.02$ (left) and the determined radii (right).

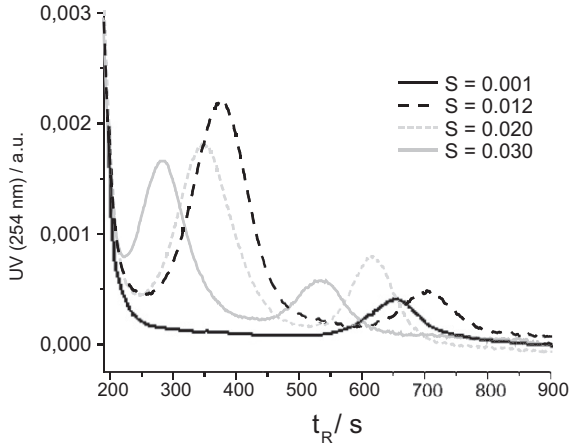

fleet ratio	AF-FFF	
	$R_{h,1}$ / nm	$R_{h,2}$ /nm
0.001	-	**62.8**
0.012	**29.1**	**72.3**
0.020	**24.4**	**60.4**
0.030	**16.1**	**50.5**

Fig. 5. Variation of the fleet ratio S and the impact on the determined particle sizes by AF-FFF for acid catalyzed polyorganosiloxane nanoparticles at $T = 293$ K and $U = 300$ rpm (left) and corresponding radii (right).

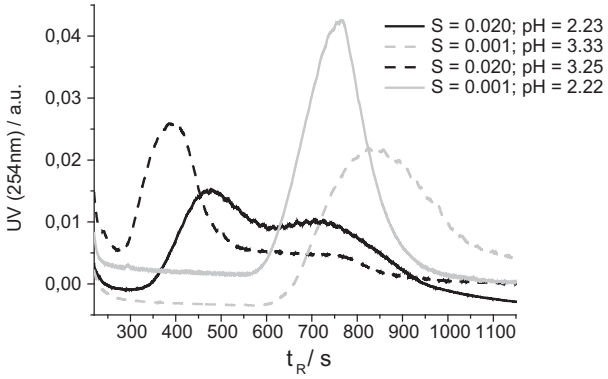

fleet ratio S	pH	AF-FFF	
		$R_{h,1}$ / nm	$R_{h,2}$ /nm
0.020	**2.23**	**24.0**	**40.3**
0.001	**3.33**	-	**47.9**
0.020	**3.35**	**18.1**	**40.9**
0.001	**2.22**	-	**43.3**

Fig. 6. Influence of the reaction pH on the size of acid catalyzed polyorganosiloxane nanoparticles as analyzed by AF-FFF at $T = 293$ K, $U = 300$ rpm and $S = 0.02$ or $S = 0.001$ with the sodium salt of dodecylphenylsulfonic acid (NaDBS) and appropriate addition of hydrochloric acid to adjust the pH (left), and determined radii (right).

defined as the mass of surfactant in relation to the mass of total monomer added $S = m_S/m_m$, with m_S: mass of surfactant, m_m: total mass of monomer, and iv) the pH.

Fig. 3 shows the AF-FFF fractograms of the samples obtained at different reaction temperatures between 20° and 70 °C. Increasing the temperature up to 80 °C leads to an unstable system and no nanoparticles are obtained. It can be seen that the bimodality of the system is not affected but an influence on the size can be observed. With increasing temperature the radii of the poly(organosiloxane) particles are increasing, which can be attributed to the change in interfacial properties of the system.

The influence of the stirrer speed during the formation of the core was analyzed by using a disperser (IKA ultra-turrax) at different stirrer speeds. Fig. 4 shows the results. It can be clearly seen that the bimodality vanishes with increasing stirrer speed until at a speed of 14000 rpm a monomodal distribution is obtained, resembling the size of the smaller particle fraction.

The change of the fleet ratio and the impact on the determined particle sizes by AF-FFF is presented in Fig. 5. As expected, the decrease in surfactant mass leads to an increase in average particle sizes, but this is observed for both species. If the fleet ratio is decreased further to $S = 0.001$ close to the limit of instability,

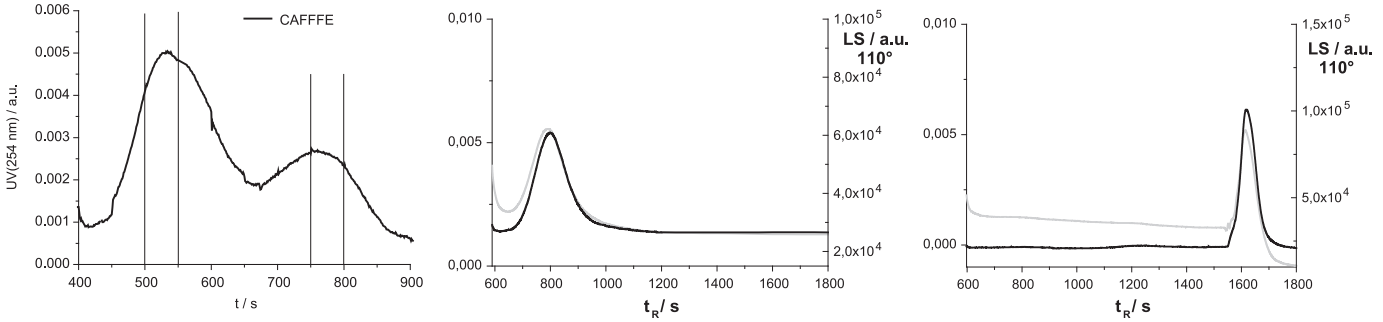

Fig. 7. Fractionation of a bimodal sample ($S = 0.02$, $T = 293$ K, $U = 300$ rpm) by CAFFFE (fractions indicated) and re-injected fractions in AF-FFF (UV($\lambda = 254$ nm): grey, light scattering at 110°: black).

Table 3
Radii of the fractions obtained by CAFFFE of acid catalyzed polyorganosiloxane nanoparticles ($S = 0.02$, $T = 293$ K, $U = 300$ rpm) and analyzed by AF-FFF and DLS. In addition, the second cumulant μ_2 (obtained at 90° scattering angle) determined from DLS is shown. Values smaller than 0.05 indicate narrow size distributions.

fraction	R_h (AF-FFF)	$R_{h,\ app}$ (DLS)	μ_2
small spheres	24.7 nm	25.9 nm	0.041
large spheres	62.0 nm	54.3 nm	0.005

a monomodal size distribution resembling the larger spheres is obtained. This is discussed in more detail below. It should be added that it has been shown that the surface of the polyorganosiloxane nanoparticles in aqueous dispersion (base catalysis) is not fully covered with surfactant, but partly self-stabilized by silanol and silanolate groups, which leads to the inapplicability of e.g. microemulsion theory [26].

The influence of the reaction pH was analyzed by employment of the sodium salt of the surfactant and addition of the appropriate amount of hydrochloric acid neglecting the potential influence of the minor increase of the ionic strength, which has been shown previously to be negligible [27]. The corresponding AF-FFF fractograms obtained after addition of the monomer mixtures of the first and second shell are shown in Fig. 6. A slight influence on the resulting average particle sizes can be seen, but basically the results are comparable to the different fleet ratios as discussed above.

In order to investigate whether the observed changes especially upon change of the fleet ratio could in principle be attributed to a potential secondary nucleation as already observed in different sample preparations before [26], the aqueous dispersion of the bimodal sample with $S = 0.02$ was fractionated using a CAFFFE system in order to obtain the two different size fractions for further analysis (Fig. 7).

To determine the effectiveness of the separation of the bimodal poly(organosiloxane) nanospheres, fractions of each peak were collected and re-injected in a classical AF-FFF channel (also shown in Fig. 7). Based on the flow rates used and the observed peak widths, a sample dilution of approximately 1:100 can be estimated for the CAFFFE system, resulting in a typical sample load used in classical AF-FFF. The obtained fractograms of the two fractions are comparable to the original fractogram of the bimodal sample and do not contain nanospheres of the respective other fraction. DLS measurements of the individual fractions revealed besides the comparable hydrodynamic radii the narrow distribution of both particle sizes (Table 3). TEM pictures obtained from the original sample and the two individual fractions (Fig. 8) also confirm these results.

To investigate the core material of each fraction, an ultrafiltration cell equipped with a regenerated cellulose membrane (MWCO = 30 kDa) was used to separate the core material from the particles. The obtained material was analyzed with MALDI-TOF and gas chromatography (SI, Figure S1). MALDI-TOF experiments reveal that linear polydimethylsiloxane chains with average molecular weights of approximately $M = 1300$ g/mol are present in the core material of the small population while they are absent in case of the larger fraction. Also the chromatograms obtained by GC measurements provide an objective evidence for this assumption. It is observed that again only in the smaller particles PDMS chains are formed, represented by the homologous series in the chromatogram and MALDI-TOF spectrum, besides the cyclic condensation products. On the other hand, in the chromatogram of the fraction containing the large population the amount of cyclic condensation products is strongly increased and no PDMS chains could be detected.

Obviously, the origin of the bimodality can already be attributed to the synthesis of the core. In order to investigate this in more detail, the experiment has been slightly modified to yield sufficient material for ^{29}Si-NMR analysis. Therefore, 0.05 g DBS (10% (w/w)), 5 g D and 1.25 g water (instead of 5 g DBS (10% (w/w)), 5 g D and 125 g water) were mixed directly in the NMR tube. The obtained ^{29}Si-NMR spectrum (Fig. 9) reveals that besides linear chains (polydimethylsiloxane (PDMS)) also cyclic condensation products (mainly octamethyltetracyclosiloxane (D4) and decamethylpentacyclosiloxane (D5), and higher cycles) are formed.

With increasing reaction time a phase separation within the reaction mixture can be observed (SI, Figure S2). While the lower phase consists only of the cyclic condensation products the upper phase showed linear PDMS chains in addition. Quantitative analysis of the data of the upper phase yields a fraction of 20% (w/w) of chains compared to 80% of cyclic products. Although the synthesis had to be modified to the detection limit of NMR, the results indicate that also in the originally prepared dispersion of the core different types of nanoemulsions are formed and induce the observed bimodality of acid catalyzed poly(organosiloxane) nanospheres. Introduction of the separated fractions into the typically continued nanoparticles synthesis leads to the formation of smaller particles for the upper phase (average radius of 12 nm) and larger nanoparticles (radius approximately 36.5 nm) for the lower phase (data not shown). If a lower amount of surfactant (0.0025 g DBS (10% (w/w)) is used or higher stirrer speed ($U = 14000$ rpm), no phase separation is observed and higher amount of PDMS is determined by ^{29}Si-NMR (data not shown).

To further elucidate this assumption, appropriate mixtures of commercially available PDMS ($M = 1250$ g/mol) and D4 and D5 have been used to mimic the core of the polyorganosiloxane nanoparticles during the beginning of the synthesis. The results obtained by AF-FFF show that the particle radii slightly increase with decreasing amount of PDMS (Fig. 10, Table 4). At a ratio of 20% (w/w) PDMS and 80% of cyclic structures, an asymmetrical distribution with smaller particles of approximately 23 nm and a pronounced tailing to larger sizes is observed, corresponding nicely to the results discussed above.

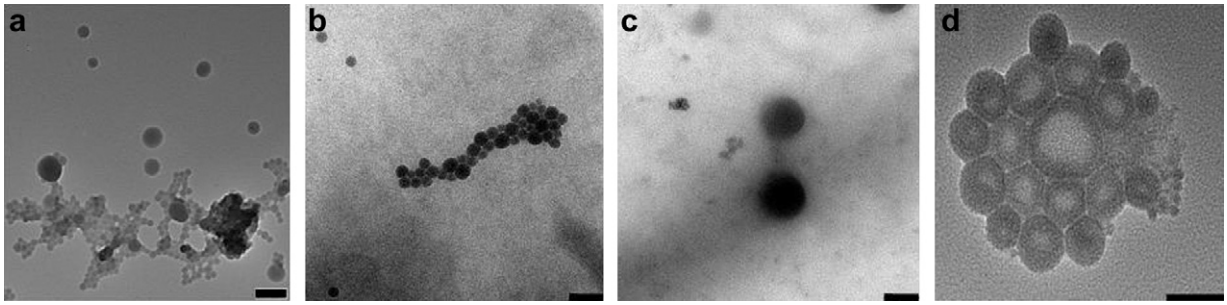

Fig. 8. TEM pictures of the acid catalyzed polyorganosiloxane nanoparticles ($S = 0.02$, $T = 293$ K, $U = 300$ rpm) from aqueous dispersion before (a) and after (b, c) fractionation by CAFFFE, and from toluene after end-capping without fractionation (d), from left to right; scale bar 100 nm.

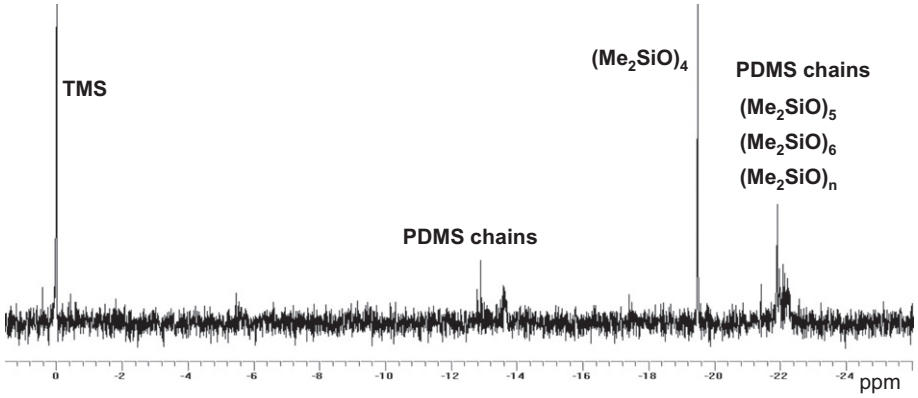

Fig. 9. ^{29}Si-NMR spectrum of the modified acid catalyzed reaction of diethoxydimethylsilane in water with DBS at the beginning of the reaction.

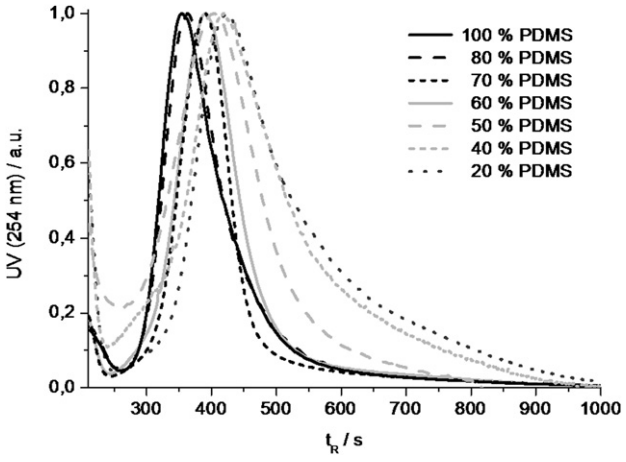

Fig. 10. Mixtures of commercially available PDMS ($M = 1250$ g/mol) and D4 and D5 have been used to mimic the core of the polyorganosiloxane nanoparticles during the core formation of acid catalyzed polyorganosiloxane nanoparticles ($S = 0.02$, $T = 293$ K, $U = 300$ rpm). Normalized AF-FFF fractograms of the aqueous dispersions after addition of the monomers for the second shell.

The theory of miniemulsion describes the stabilization of oil droplets against Ostwald ripening by employment of an ultrahydrophobe in addition to a surfactant [28]. This description can be used to understand the evolution of the bimodal size distribution in our system. The smaller sized particles contain the ultrahydrophobe PDMS, whereas the larger particles are only stabilized by the surfactant. The stabilization of the smaller particles is the result of the balance between Laplace pressure and osmotic pressure, as expressed in terms of the pressure difference (Δp): [28]

Table 4
Radii of the acid catalyzed polyorganosiloxane nanoparticles with pre-mixed core of PDMS, D4 and D5 after formation of the second shell ($S = 0.02$, $T = 293$ K, $U = 300$ rpm) as determined by AF-FFF and DLS. The μ_2 values obtained at 90° indicate a pronounced increase in polydispersity at a PDMS content in the core forming mixture lower than 60% (w/w).

PDMS	AF-FFF	DLS	
w-%	R_h/nm	R_h/nm	μ_2
100	10.8	11.2	0.04
80	11.3	14.3	0.04
70	13.7	14.9	0.03
60	15.9	15.2	0.05
50	16.0	16.2	0.10
40	23.4	21.1	0.17
20	23.2	24.9	0.17

$\Delta p = \frac{2\sigma}{R} - \frac{3nkT}{4\pi R^3}$, with σ: interface tension, R: particle radius, n: number of ultrahydrophobes, k: Boltzmann's constant, T: absolute temperature.

The larger spheres are stabilized by the surface tension based on the presence of hydrophilic moieties of the siloxane network such as silanol and silanolate groups and the surfactant. Therefore, increase of temperature leads to decrease of stabilization properties of the surfactant and thus to increase in particle radius. Decrease of the amount of surfactant results in lack of stabilizing surfactant and larger particles are formed. Increase of stirrer speed or shear forces seems to lead to an increase in the number of PDMS chains built and therefore to a predominant stabilization of the smaller spheres. The reaction pH between 2.2 and 3.4 seems to have only minor influence. Overall, the observed behavior is – though relatively complex – comparable to miniemulsions.

5. Conclusion

The origin of the observed bimodal size distribution during the acid catalyzed synthesis of core-shell-shell polyorganosiloxane nanoparticles with extractable PDMS core is attributed to a reaction driven self organization during formation of the core, which can be described by a miniemulsion approach. The reaction leads to the inherent nanoseparation into small nanoparticles having radii of approximately 26 nm with cores consisting of PDMS chains and cyclic products, and larger nanoparticles of 60 nm in size, which cores possess only cyclic products. The size of the nanoparticles can be fine-tuned and is influenced by the temperature, the stirrer speed, the pH and mainly by the amount of surfactant added. Monomodal size distributions are obtained by either drastic increase of the stirrer speed, leading to nanoparticles of 21.8 nm in radius, or by decrease of the amount of surfactant leading to nanoparticles having radii of 62.8 nm. In the future, this will be used to synthesize hydrido-functionalized nanoparticles, which can be subsequently further modified by hydrosilation reactions.

Acknowledgments

The financial support of the BAM Federal Institute for Materials Science and Testing for C.S. and from DFG SPP 1313 is gratefully acknowledged. We thank J. Venzmer and C. Bockmann, Evonik Goldschmidt GmbH, for help with the GC measurements.

Appendix A. Supplementary material

Supplementary data associated with this article can be found, in the online version, at doi:10.1016/j.polymer.2010.09.065.

References

[1] Barbe C, Bartlett J, Kong L, Finnie K, Lin HQ, Larkin M, et al. Adv Mater 2004;16:1959–66.
[2] Singh M, Briones M, Ott G, O'Hagan D. Proc Natl Acad Sci U.S.A 2000;97:811–6.
[3] Roy I, Ohulchanskyy TY, Bharali DJ, Pudavar HE, Mistretta RA, Kaur N, et al. Proc Natl Acad Sci U.S.A 2005;102:279–84.
[4] Bharali DJ, Klejbor I, Stachowiak EK, Dutta P, Roy I, Kaur N, et al. Proc Natl Acad Sci U.S.A 2005;102:11539–44.
[5] Roy I, Ohulchanskyy TY, Pudavar HE, Bergey EJ, Oseroff AR, Morgan J, et al. J Am Chem Soc 2003;125:7860–5.
[6] Wang C, Ge Q, Ting D, Nguyen D, Shen HR, Chen JZ, et al. Nat Mater 2004;3:190–6.
[7] Zhu MQ, Zhu LY, Han JJ, Wu WW, Hurst JK, Li ADQ. J Am Chem Soc 2006;128:4303–9.
[8] Ow H, Larson DR, Srivastava M, Baird BA, Webb WW, Wiesner U. Nano Lett 2005;5:113–7.
[9] Beydoun D, Amal R, Low G, McEvoy S. J Nanoparticle Res 1999;1:439–58.
[10] Kaltenpoth G, Himmelhaus M, Slansky L, Caruso F, Grunze M. Adv Mater 2003;15:1113–8.
[11] Jang J, Nam Y, Yoon H. Adv Mater 2005;17:1382–6.
[12] Unger KK, Kumar D, Grun M, Buchel G, Ludtke S, Adam T, et al. J Chromatogr A 2000;892:47–55.
[13] Yi DK, Lee SS, Papaefthymiou GC, Ying JY. Chem Mater 2006;18:614–9.
[14] Utech S, Scherer C, Krohne K, Carella L, Rentschler E, Gasi T, et al. J Magn Magn Mater 2010;322:3519–26.
[15] Stober W, Fink A, Bohn E. J Colloid Interface Sci 1968;26:62–9.
[16] Nozawa K, Gailhanou H, Raison L, Panizza P, Ushiki H, Sellier E, et al. Langmuir 2005;21:1516–23.
[17] Jungmann N, Schmidt M, Maskos M, Ebenhoch J, Weis J. Macromolecules 2002;35:6851–7.
[18] Utech S, Scherer C, Maskos M. J Magn Magn Mater 2009;321:1386–8.
[19] Graf C, Schaertl W, Maskos M, Schmidt M. J Chem Phys 2000;112:3031–9.
[20] Jungmann N, Schmidt M, Ebenhoch J, Weis J, Maskos M. Angew Chem Int Ed Engl 2003;42:1714–7.
[21] Jungmann N, Schmidt M, Maskos M. Macromolecules 2003;36:3974–9.
[22] Diehl C, Fluegel S, Fischer K, Maskos M. Progr Poly Coll Sci 2008;134:128–33.
[23] Maskos M, Schupp W. Anal Chem 2003;75:6105–8.
[24] McNeil KJ, Walsh DA, Pratt RF. J Am Chem Soc 1980;102:1859–64.
[25] Emmerich O, Hugenberg N, Schmidt M, Sheiko S, Baumann F, Deubzer B, et al. Adv Mater 1999;11:1299.
[26] Jungmann N, Schmidt M, Maskos M. Macromolecules 2001;34(23):8347–53.
[27] Baumann F. Ph.D. thesis. Germany: University of Bayreuth; 1995.
[28] Landfester K. Macromol Rapid Commun 2001;22:896.